

Vortex–glass state in the isovalent optimally doped pnictide superconductor



This content has been downloaded from IOPscience. Please scroll down to see the full text.

2017 Supercond. Sci. Technol. 30 055003

(<http://iopscience.iop.org/0953-2048/30/5/055003>)

View [the table of contents for this issue](#), or go to the [journal homepage](#) for more

Download details:

IP Address: 159.226.35.171

This content was downloaded on 18/08/2017 at 03:02

Please note that [terms and conditions apply](#).

You may also be interested in:

[Flux-flow and vortex-glass phase in iron pnictide \$\text{BaFe}_2\text{-xNixAs}_2\$ single crystals with \$T_c\$ 20 K](#)
S Salem-Sugui Jr, A D Alvarenga, H-Q Luo et al.

[Vortex-glass transformation within the surface superconducting state of \$\gamma\$ -phase \$\text{Mo}_{1-x}\text{Re}_x\$ alloys](#)
Shyam Sundar, M K Chattopadhyay, L S Sharath Chandra et al.

[Thermally activated transport and vortex-glass phase transition of \$\text{K}_{0.78}\text{Fe}_{1.70}\text{Se}_2\$ single crystals](#)
Yi Yu, Chunchang Wang, Qiuju Li et al.

[Vortex-glass phase transition and enhanced flux pinning in \$\text{C}_4^+\$ -irradiated \$\text{BaFe}_{1.9}\text{Ni}_{0.1}\text{As}_2\$ superconducting single crystals](#)
M Shahbazi, X L Wang, S R Ghorbani et al.

[Observation of an anomalous peak in isofield \$M\(T\)\$ curves in \$\text{BaFe}_2\(\text{As}_{0.68}\text{P}_{0.32}\)_2\$ suggesting a phase transition in the irreversible regime](#)
S Salem-Sugui Jr, J Mosqueira, A D Alvarenga et al.

[TAFF and vortex glass state in a niobium oxy-nitride \$\text{Nb}\(\text{N}_{0.98}\text{O}_{0.02}\)\$](#)
D Venkateshwarlu, V Ganesan, Y Ohashi et al.

[Crystal structure and superconducting properties of hole-doped \$\text{Ca}_{0.89}\text{Na}_{0.11}\text{FFeAs}\$ single crystals](#)
L Shlyk, K K Wolff, M Bischoff et al.

Vortex–glass state in the isovalent optimally doped pnictide superconductor $\text{BaFe}_2(\text{As}_{0.68}\text{P}_{0.32})_2$

S Salem-Sugui Jr¹, J Mosqueira², A D Alvarenga³, D Sóñora², A Crisan⁴, A M Ionescu^{4,5}, S Sundar¹, D Hu⁶, S-L Li⁶ and H-Q Luo⁶

¹Instituto de Física, Universidade Federal do Rio de Janeiro, 21941-972 Rio de Janeiro, RJ, Brazil

²LBTS, Universidade de Santiago de Compostela, E-15782, Spain

³Instituto Nacional de Metrologia Qualidade e Tecnologia, 25250-020 Duque de Caxias, RJ, Brazil

⁴National Institute of Materials Physics Bucharest, 405A Atomistilor Str., 077125 Magurele, Romania

⁵Faculty of Physics, University of Bucharest, 077125 Bucharest-Magurele, Romania

⁶Beijing National Laboratory for Condensed Matter Physics, Institute of Physics, Chinese Academy of Sciences, Beijing 100190, People's Republic of China

E-mail: said@ifufrj.br

Received 2 January 2017, revised 6 February 2017

Accepted for publication 24 February 2017

Published 23 March 2017



CrossMark

Abstract

We report on isochamp magneto-resistivity and ac susceptibility curves obtained in a high-quality single crystal of the isovalent optimally doped pnictide $\text{BaFe}_2(\text{As}_{0.68}\text{P}_{0.32})_2$ with superconducting temperature $T_c = 27.8$ K for $H \parallel c$ -axis. Plots of the logarithmic derivative of the resistivity curves allowed the identification of a vortex–glass (VG) phase and to obtain the values of the critical glass temperature T_g , the temperature T^* marking the transition to the liquid phase and of the critical exponent s . The presence of the VG phase is confirmed by detailed measurements of the third harmonic signal of the ac magnetic susceptibility. The modified VG model was successfully applied to the data allowing the obtention of the temperature independent VG activation energy U_b . The activation energy U_0 obtained from the Arrhenius plots in the flux–flow region are compared with U_b and with U_0 obtained from flux–creep measurements on a $M(H)$ isothermal in the same sample. A phase diagram of the studied sample is constructed showing the T_g glass line, the T^* line representing a transition (melting) to the liquid phase, the mean field temperature $T_c(H)$ line and the H_p line obtained from the peaks in isothermal critical current, $J_c(H)$ curves, which are explained in terms of a softening of the vortex lattice. The glass line was fitted by a theory presented in the literature which considers the effect of disorder.

Keywords: superconductor pnictide, vortex–glass state, pinning activation energy, critical current

(Some figures may appear in colour only in the online journal)

1. Introduction

A rich variety of phenomena have been observed in the vortex state of type II superconductors, where in most cases the distribution and energy of pinning sites play an important role. Among these phenomena, one which received great attention is the transition occurring in the vortex state as it approaches the reversible region, which can be either first

order when a melting in the vortex lattice occurs or second order when the vortex liquid approaches a vortex–glass (VG) irreversible phase as the temperature is reduced [1]. The VG phase, which depends on the disorder has been predicted in [2] as a possible phase occurring in the high- T_c superconductors [3, 4], and since then it has been observed and studied in many type II superconductors [1, 5]. A characteristic critical behaviour predicted for this phase is that the

resistivity in the flux–flow liquid region should approach zero as the temperature approaches the glass temperature T_g following a power law behaviour $|T - T_g|^s$ where s is a combined glass critical exponent. In addition to the above prediction for the VG phase occurring below T_g , a modified VG model was developed in [6, 7] to study the VG phase in the high- T_c superconductors. This model assumes that the VG pinning energy should scale with $k_B T_g$ where k_B is the Boltzmann constant, and defines the VG activation energy $U_0 = k_B T_g$. As shown in [6, 7] this modified VG model allows the detailed study of the VG phase as it predicts new equations and relations that should be followed by the resistivity and U_0 in the vicinity of T_g , and also allows the extraction of the temperature independent VG activation energy U_b .

The search and study of the VG phase in iron-pnictides [8–10] appears to be still restricted to a few works, but it is gaining increasing attention. So far, the VG phase has been observed and studied in $(\text{Ba,K})\text{Fe}_2\text{As}_2$ [11, 12]; $\text{Ba}(\text{Fe}, \text{TM})_2\text{As}_2$ with $\text{TM} = \text{Ni}, \text{Co}$ [12–18], $\text{SmFeAsO}_{0.85}$ [19], and in the chalcogenide $\text{Fe}_{1.01}\text{Te}_{0.62}\text{Se}_{0.38}$ [20]. Out of these, the modified VG model has been applied with success to the study of the VG phase in pnictide crystals $(\text{Ba,K})\text{Fe}_2\text{As}_2$, $\text{Ba}(\text{Fe}, \text{Co})_2\text{As}_2$ and $\text{Ba}(\text{Fe}, \text{Ni})_2\text{As}_2$ [12, 14, 18]. However, there is a lack of research on searching for the VG phase in isoavalently substituted materials like $\text{BaFe}_2(\text{As}, \text{P})_2$. Here we address this issue through measurements of the magnetoresistance around T_c in a high quality single crystal of this compound with $T_c = 27.8$ K and a transition width $\delta T_c < 1$ K, previously used in magnetic relaxation measurements [21]. The data are complemented with ac susceptibility measurements, focusing on the third harmonic, which is sensitive to the non-linear dissipation of the VG phase. The analysis of the resistivity curves allowed the observation of a distinct critical behavior associated with the VG phase and the determination of T_g as a function of H . The flux–flow region was interpreted in terms of the thermally assisted flux–flow model (TAFF) [22], allowing the extraction of values of the corresponding activation energy, U_0 . The modified VG model was applied to the resistivity curves producing isochamp curves of the VG activation energy, from which it was possible to extract values of T_g , U_b and also of a temperature $T_a(H)$ which is close to $T_c(H)$. The TAFF U_0 and U_b were compared with the activation energy U_0 obtained from flux–creep measurements in the same sample [21]. Critical current, $J_c(H)$ curves are obtained from previous measurements [21] and the peak, H_p , in each curve is explained in terms of a softening of the vortex lattice, further suggesting an order–disorder transition occurring near the H_p line above which the VG phase develops. The T_g line was fitted by a theory developed in [23] which takes in to account the effect of disorder.

2. Experimental

We measured a high-quality single crystal of $\text{BaFe}_2(\text{As}_{0.68}\text{P}_{0.32})_2$ with approximate dimensions of

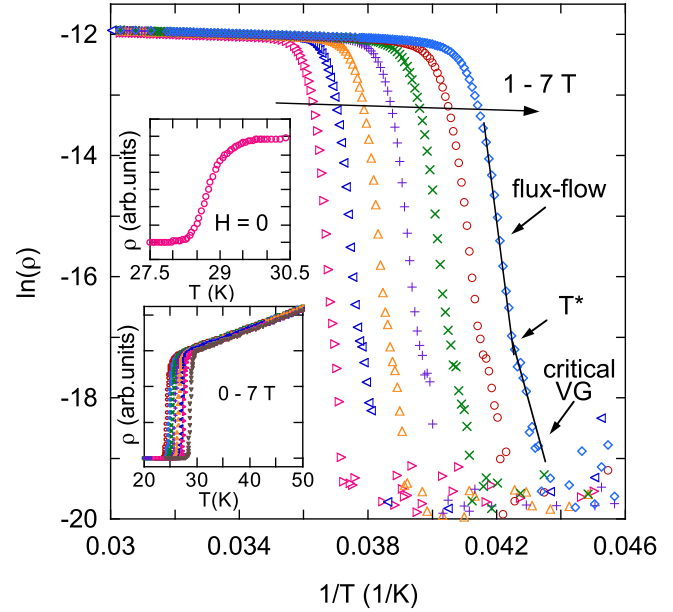


Figure 1. $\ln(\rho)$ is plotted against $1/T$. Solid lines in the 7 T data curve evidence the two different regions, flux–flow and VG region. The upper inset shows the superconducting transition and the lower inset the original resistivity curves plotted in the main figure.

$2 \times 3 \times 0.05$ mm³ and mass $m = 1.746$ mg. The crystal was grown by the BaAs/BaP flux method [24]. The sample exhibits a sharp $T_c = 27.8$ K with $\delta T_c < 1$ K. Isochamp resistivity data were obtained by the standard four probe, ac (71 Hz) lock-in technique, with the current (1 mA) flowing along the ab-planes of the sample. A Quantum Design PPMS system was used for resistivity and for ac susceptibility measurements, where the magnetic field was applied parallel to the c -axis of the sample. Resistivity was measured in a ZFC mode, by increasing temperature, while magnetic susceptibility was measured in FC mode, by decreasing temperature. We mention that all results concerning the VG phase (T_g and T^*), the VG and the flux–flow activation energies and the $T_c(H)$ crossover line were obtained from resistivity and ac susceptibility data measured in this work, while the isothermal critical current curves and flux–creep activation energy were obtained by using isothermal $M(H)$ curves and magnetic relaxation data previously published in [21] in the same sample. It is worth mentioning that both the flux–creep activation energy as well the isothermal critical current curves discussed here were not discussed or even shown in the previously published work [21].

3. Results and discussion

Figure 1 shows a plot of $\ln\rho$ versus $1/T$ exhibiting the usual linear behaviour observed in the flux–flow region which is commonly explained in terms of the TAFF model with $\ln\rho = \ln\rho_0 - U_0/k_B T$, where k_B is the Boltzmann constant and U_0 is the TAFF activation energy. The upper inset of figure 1 shows the superconducting transition for $H = 0$ T, and the lower inset shows a plot of ρ versus T as obtained for

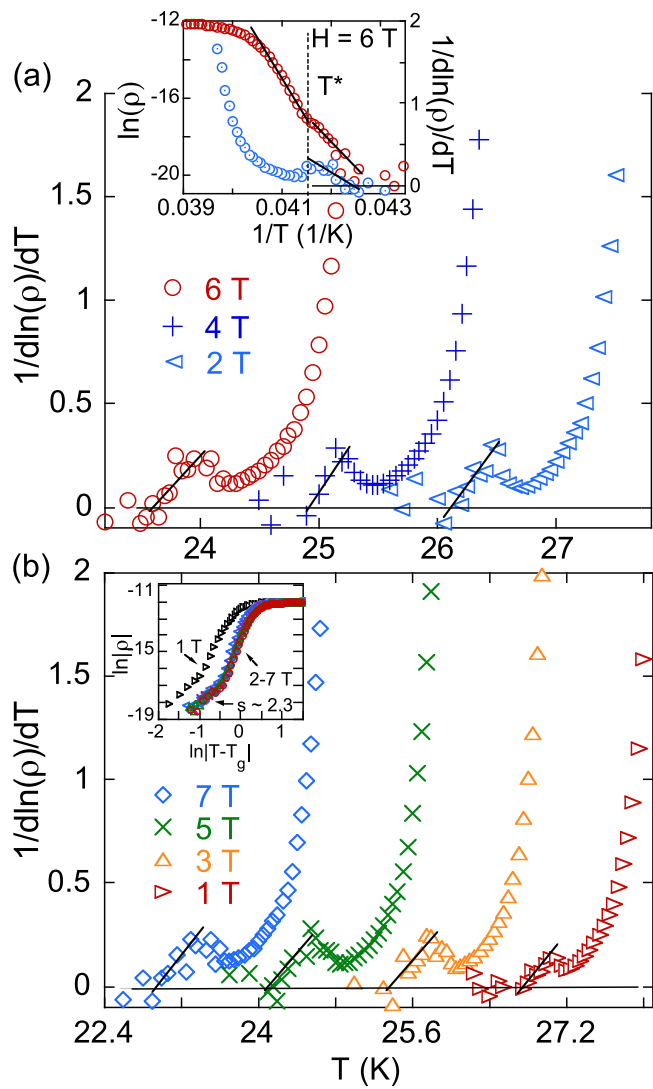


Figure 2. The inverse of the logarithmic derivative of resistivity is plotted against temperature. Solid lines are only a guide for the eyes evidencing the critical region in each curve. The inset of figure 2(a) shows a selected double plot of $\ln(\rho)$ and $1/d(\ln(\rho))/dT$ versus $1/T$, and the inset of figure 2(b) a plot of $\ln\rho$ versus $\ln|T - T_g|$.

all fields, evidencing the non-Fermi-liquid behaviour of ρ in the normal region. It is worth noting that the lower part of the curves in figure 1 change the behaviour above $1/T^*$ (indicated by an arrow) to a slightly smaller slope region developing as ρ approaches zero, a change that is found to be associated with a critical behaviour of the resistivity observed as temperature approaches T_g .

The resistivity near the VG phase is expected to obey the expression

$$\rho = \rho_n |(T - T_g)/T_g|^s, \quad (1)$$

where T_g is the glass transition temperature, ρ_n is the normal resistivity and s is a combined glass critical exponent. Figure 2 shows plots of the inverse logarithmic derivative of ρ (T). It is worth noting that the curves in figure 2 show a distinct linear region approaching zero, which is identified as the power law behaviour expected as temperature approaches

the critical temperature T_g , allowing us to obtain the values of $T_g(H)$, of the temperature T^* above which the vortex liquid state develops, and of the exponent s . Due to the scattering of the data, the values of the exponent s for the different field curves are found to vary between 2.0 and 2.5, corresponding to an average value of $s = 2.3$. The inset of figure 2(a) shows a double plot of $\ln\rho$ versus $1/T$ and of the inverse logarithmic derivative of ρ versus $1/T$, where it can be seen that the lower slope regions of the curves in figure 1 (occurring above the temperature T^* indicated by an arrow) corresponds to the linear regions (VG critical behaviour) shown in figure 2. To check for the distinct behaviour of the VG region when compared with the flux-flow one, we plotted the dependencies of $\ln\rho$ versus $\ln|T - T_g|$, which are shown in the inset of figure 2(b). It can be seen that a large number of curves at fields $H \geq 2$ T are practically collapsing in one curve, clearly showing the existence of two different regions where the small region with a lower slope corresponds to the VG critical region with an exponent $s \sim 2.3$. It should be mentioned that even if the curve for 1T does not fall in the collapsing curve, it shows the same behaviour with a value of $s = 2.3$. The value of the exponent $s \sim 2.3$ found here is smaller than the value predicted for the VG phase [2], $s = 2.7$. A similar low value of the exponent s was observed for $\text{SmFeAsO}_{0.85}$ [19], but with s decreasing as H increased. This was claimed to be a possible crossover to a 2D-like behaviour induced by the field as observed in the Bi-cuprates, but it is not the case here as the values of the exponent s do not show a field dependence. Also, the doped BaFe_2As_2 systems are known to be 3D in nature, so probably the values of the exponent s found here might be accommodating within a lower limit value of the exponent s representing a VG phase in pnictides.

The transition between VG and vortex liquid can also be determined from ac susceptibility measurements with very small perturbation (very small probing current, hence, very small ac field amplitude) [25]. The principles of this matter come from the very basic properties of vortex matter: for sufficiently low currents, in the VG phase the dissipation is strongly non-linear, while for the vortex liquid phase, the dissipation is ohmic, hence linear. At the same time, it is well known that the out-of-phase susceptibility is a measure of the total dissipation (linear plus non-linear), while the third harmonic is a measure of the non-linear dissipation only [26]. Experimentally, we have probed the VG-vortex liquid transition by measuring the temperature dependence of both fundamental out-of-phase susceptibility and third harmonic susceptibility. At the onset temperature of the out-of-phase susceptibility the sample enters the superconducting state, while at a lower temperature T_g , the onset of third harmonic susceptibility reflects the appearance of non-linear dissipation, hence the appearance of VG. As the literature is lacking on third harmonic studies associated with the VG phase in pnictides, we performed a detailed study of the ac susceptibility response in our sample, for which the VG phase is well identified (see figure 2). The study was performed by obtaining isochamp ac susceptibility for several frequencies and amplitudes of the ac magnetic field. Figure 3(a) shows double plots of selected isochamp susceptibility

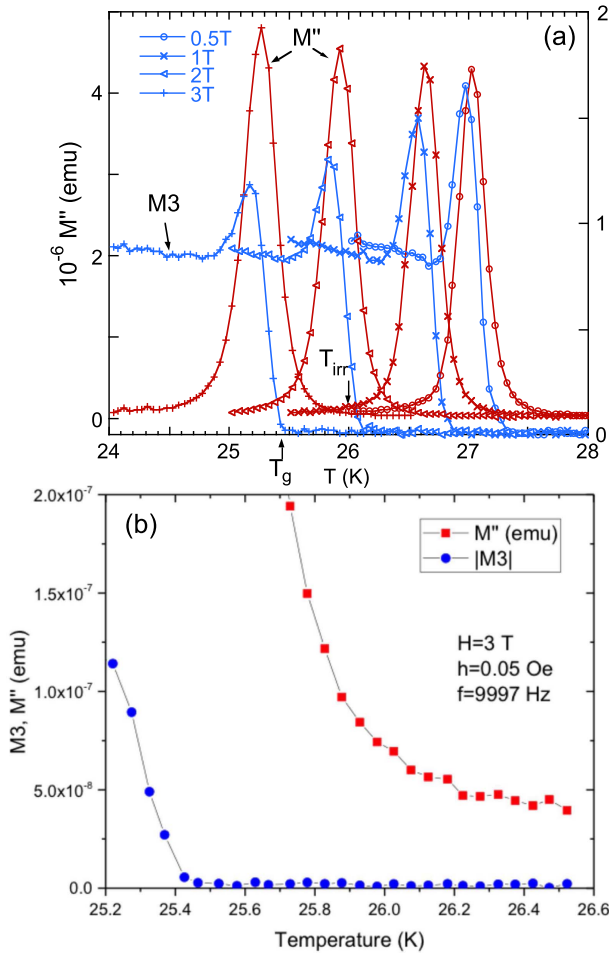


Figure 3. (a) Double plot of M'' and $M3$ (third harmonic) as a function of temperature for selected fields. (b) The temperature dependence of the out-of-phase (M'') and third harmonic ($M3$) magnetic response in a DC field of 3 T, at a low ac field excitation of 0.05 Oe and frequency of 9997 Hz. It can be seen that the difference in the two onsets is more than 0.5 K.

measurements obtained for a 9997 Hz frequency and 0.05 Oe ac magnetic field, where the out-of-phase part of the ac susceptibility M'' is plotted along with the third harmonic magnetic response, $M3$, against temperature. As expected the curves in figure 3(a) show that the onset of the non-linear dissipation, shown by an arrow in the $M3$ curve for $H = 3$ T, does not coincide with the corresponding onset of linear dissipation in M'' curves, similar to what have been observed in the high- T_c superconductors [25]. This can be seen more clearly in figure 3(b), which is in fact an enlargement close to the onset of the two curves for 3 T. As expected the onset of the non-linear dissipation observed in each $M3$ curve marks the onset of the VG state as these values obtained from the isochamp $M3$ curves going from 0.5 T to 7 T almost coincide with values of T_g obtained from figure 2.

As already mentioned, the modified VG model assumes that $k_B T_g = U_0$, where U_0 is the VG activation energy. By replacing $T/T_g = k_B T/U_0$ in equation (1) the authors in [7] obtained

$$U_0(H, T) = k_B T [1 + (\rho/\rho_n)^{1/s}]^{-1}. \quad (2)$$

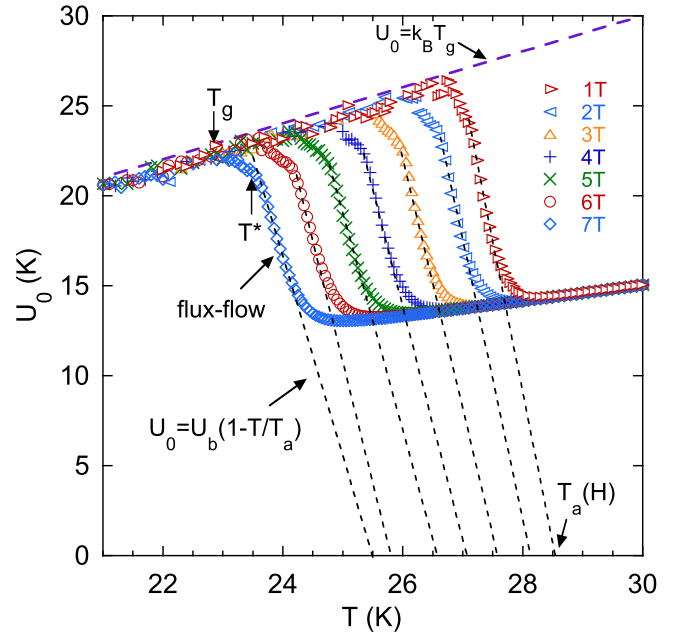


Figure 4. Plot of U_0 versus T as obtained from the modified VG model. The dotted lines are guides for the eyes.

Figure 4 shows isochamp plots of U_0 versus T calculated by using equation (2). The curves in figure 4 show a different behaviour with temperature when compared with similar curves obtained in optimally doped $YBa_2Cu_3O_{7-x}$ [7] and $Ba(Fe,Ni)_2As_2$ [14, 18], as the regions obeying the power law behaviour in figure 2 show a distinct behaviour from the flux-flow region. A consequence of that is that the T_g in each curve can be found as the slightly rounded line (corresponding to the linear region shown in figure 2) encounters the straight inclined line defined by $k_B T_g = U_0$. On the other hand, the extrapolations of the lower linear regions of the curves do not encounter the T axis at T_c as in [7] and [14], but at a temperature named $T_a(H)$ which we observed to be very close to $T_c(H)$ obtained from the 90% criterion of the normal resistivity. The later was also observed in [18] for $Ba(Fe,Ni)_2As_2$. The lower linear region shown in figure 4 defines an empiric form for U_0 given by $U_0(H, T) = U_b(1 - T/T_a)$ which allows to extract values of $T_a(H)$ and of the temperature independent activation energy $U_b(H)$. It should be mentioned that this empiric form obtained for U_0 is different than that obtained in [7, 14] namely $U_0 = U_b(1 - T/T_c)$. A consequence of this is the impossibility to obtain an expression for T_g as a function of H as in [7].

Another interesting expression that can be obtained from the modified VG model is by observing that the empiric form of $U_0(H, T) = U_b(1 - T/T_a) = k_B T_g$ allows us to write $U_b = k_B T_g T_a / (T_a - T_g)$ so $U_0 = k_B T_g (T_a - T) / (T_a - T_g)$ which can be substituted in equation (2) producing a general relation for the normalised resistivity in the vicinity of the VG phase

$$\rho/\rho_n = [(T/T_g)(T_a - T_g)/(T_a - T) - 1]^s. \quad (3)$$

The above equation predicts that curves of the normalised resistivity plotted as a function of the scaled temperature

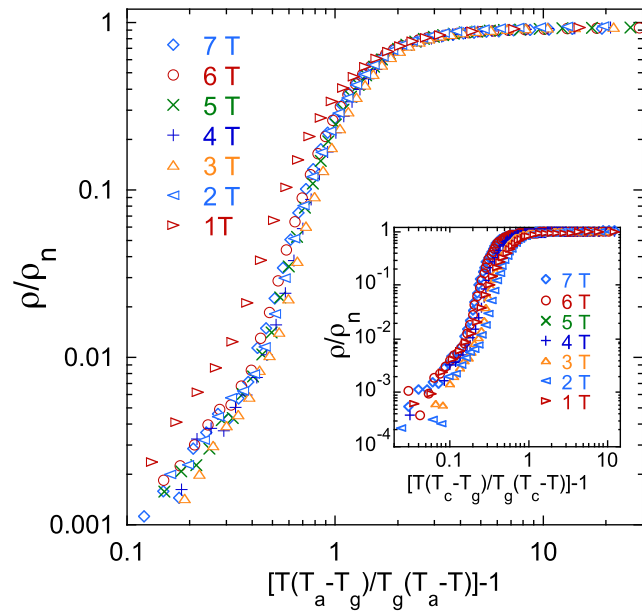


Figure 5. ρ/ρ_n is plotted versus $(T/T_g)(T_a - T_g)/(T_a - T) - 1$ in a double log plot for all applied fields. The inset shows the same plot but against $(T/T_g)(T_c - T_g)/(T_g(T_c - T)) - 1$.

$t_s = (T/T_g)(T_a - T_g)/(T_a - T) - 1$ should collapse in one single curve. Figure 5 shows a plot of the normalised resistivity as a function of t_s from which is possible to see that all curves, except the one at $H = 1$ T, collapse in one single curve. In some way the resulting curve in figure 5 is quite similar to the plot of $\ln\rho$ versus $\ln|T - T_g|$ shown in the inset of figure 2(b). To check whether the empiric form of U_0 found in [7] would produce a better result as in figure 5 we plotted in the inset of figure 5 ρ/ρ_n versus $(T/T_g)(T_c - T_g)/(T_g(T_c - T)) - 1$ where the normalised resistivity in this case was obtained by assuming the empiric form of $U_0 = U_b(1 - T/T_c)$. It can be seen that the curves in the inset of figure 5 do not collapse nicely evidencing that the empiric form of $U_0(H, T) = U_b(1 - T/T_a)$ is more appropriate.

Figure 6 shows U_0 obtained from the TAFF model, U_b obtained from the modified VG model and $U_0 (= T/R)$ obtained from the magnetic relaxation rate, R , at $T = 21$ K for the same sample [21]. It can be seen that U_0 obtained from the TAFF model is about one order of magnitude larger than U_b , but presents the same field dependence. An interesting result is that U_b is of the same order of magnitude as the one obtained from flux-creep, but presents a different behaviour since U_0 obtained from flux-creep is related to the second magnetization peak (SMP) appearing in the respective isothermal $M(H)$ [21] (see the right inset of figure 6). As previously observed in other pnictides [14, 18, 27–30], the TAFF U_0 and U_b present two different power law behaviours of the form $H^{-\alpha}$, where a weaker dependence with H is observed up to $H = 4$ T with $\alpha = 0.19$ for U_0 and 0.21 for U_b and a stronger field dependence for H above 4 T with $\alpha = 0.45$ for U_0 and 0.53 for U_b . The authors in [30] suggested that the double field dependence of U_0 shown in figure 6 is associated with a crossover from single vortex-pinning in the low field region to a small bundle pinning for higher fields. It is

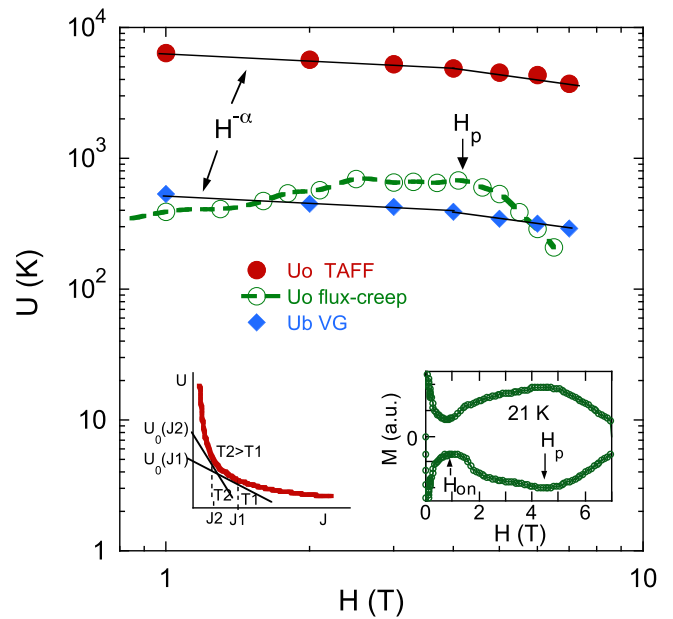


Figure 6. Several activation energies obtained for the same sample are plotted against H (double logarithmic scale). Solid lines represent power law fittings while the dotted line is a guide for the eyes. The left inset shows a characteristic plot expected for the isochamp activation energy $U(J)$, and the right inset shows the isothermal $M(H)$ obtained at 21 K from which U_0 in the main figure has been obtained.

interesting to compare U_0 (obtained from the TAFF model) and U_b in figure 6 with values obtained for the same quantities in [12] for the charge doped $(\text{Ba,K})\text{Fe}_2\text{As}_2$, $\text{Ba}(\text{Fe}, \text{Ni})_2\text{As}_2$ and $\text{Ba}(\text{Fe}, \text{Co})_2\text{As}_2$. The TAFF U_0 in figure 6 is of the same order of U_0 for $(\text{Ba,K})\text{Fe}_2\text{As}_2$, slightly larger than U_0 for $\text{Ba}(\text{Fe}, \text{Ni})_2\text{As}_2$ and more than twice as large as U_0 for $\text{Ba}(\text{Fe}, \text{Co})_2\text{As}_2$. On the other hand, U_b in figure 6 is more than twice as large than U_b found for all the three charge doped 122 systems. The right inset of figure 6 shows the isothermal $M(H)$ at 21 K exhibiting the SMP over which magnetic relaxation data were obtained. H_{on} marks the onset of the SMP and H_p is the peak position which correlates with the position of the maximum in U_0 shown in the main panel. The left inset of figure 6 shows a typical non-linear form expected for the isochamp activation energy $U(J)$ as a function of the critical current J [31, 32]. The tangent to a certain point of the curve intercepts the y-axis at the U_0 value obtained from flux-creep measurements [31, 32]. As shown in this inset, U_0 is expected to reach a very large value as J approaches zero (and T approaches T_g), so one would expect that the value of U_0 obtained from the TAFF model, which should correspond to the value of U_0 at $J = 0$ in the inset figure, should be much larger than the corresponding value of U_0 measured for the same magnetic field in the irreversible region (flux-creep) with a finite value of J . This conjecture may explain why values of U_0 obtained from the TAFF model in the reversible region are much larger than the values of U_0 found from flux-creep.

We finally present in figure 7 the phase diagram constructed from values of $T_g(H)$, $T^*(H)$, $T_a(H)$ and $T_c(H)$ obtained for our sample, where the values of $T_c(H)$ were

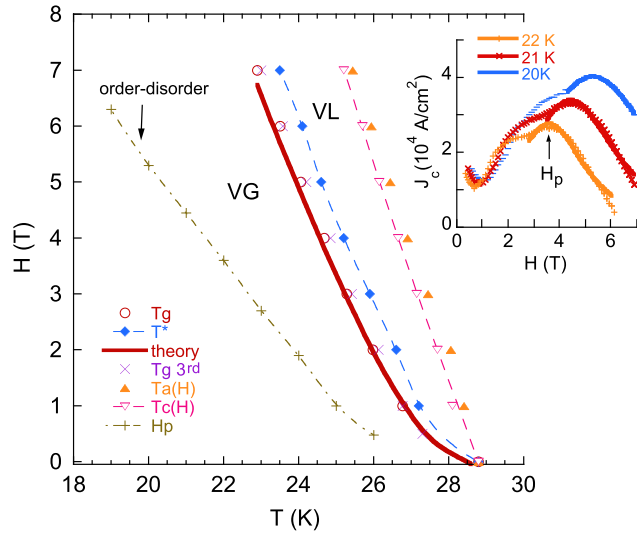


Figure 7. Magnetic phase diagram obtained from this work. The solid line is a fit of equation (4) to the T_g line while the other lines are guides for the eyes. The inset shows selected $J_c(H)$ curves where the solid lines are fits to the theory in [37].

obtained assuming that the mean field superconducting temperature occurs at the temperature corresponding to 90% of the normal resistivity. The values of $T_g(H)$ obtained from the resistivity virtually coincide with the ones obtained from the third harmonic. The very small, but systematic, difference is most likely due to the difference in the probing current in the two techniques (the transport current and the magnetically-induced current, respectively). The region between the lines formed by T_g and T^* corresponds to the region where resistivity vanishes exhibiting a power law behaviour with $|T - T_g|$, above which the vortex-liquid phase takes place. The region between T_g and T^* has been identified in [19] as a weakly entangled (pinned) vortex-liquid region. In that sense the line formed by T^* would represent a melting line. Probably due to the equipment sensitivity we could not detect any evidence of a melting transition. Figure 7 also shows that the values of $T_a(H)$ obtained from figure 3 are close to the values of $T_c(H)$ extracted from resistivity curves, where $\mu_0 dH_{c2}/dT = -1.9$ T/K. We used the WHH expression [33], $H_{c2}(0) = 0.695T_c[dH_{c2}/dT]$, to estimate the value of $\mu_0 H_{c2}(0) = 38$ T. As point disorder is fundamental for the existence of the VG phase, it is interesting to fit the T_g line in figure 7 by the expression presented below which was developed in [23] for the glass line by taking into account the effect of disorder,

$$1 - t - b + 3n_p(1 - t)^2/4\pi - 2\sqrt{2G_i}tb = 0, \quad (4)$$

where $t = T/T_c$, $b = H/H_{c2}(0)$, and the fitting parameters are $H_{c2}(0)$, n_p which measures the disorder, and G_i which is associated to the Ginzburg number measuring the strength of thermal fluctuations. The result of the fitting of equation (4) to the T_g line is also shown in figure 7 as the thick full line, where the resulting fitting parameters are $\mu_0 H_{c2}(0) = 49$ T, $n_p = 0.007$ and $G_i = 0.8 \times 10^{-5}$. This $H_{c2}(0)$ is well above the one estimated from the WHH formula, but it is important to note that it underestimates the value of $H_{c2}(0)$ for some

multiband superconductors [34, 35]. n_p is about twice as large than values found for $\text{Ba}(\text{Fe},\text{Ni})_2\text{As}_2$ [18, 36] and more than three times larger than the one found for NbSe_2 [23]. Such a large value of n_p may be responsible for the robust evidence of the VG critical region observed in figures 2 and 4. The value of G_i is about one order of magnitude larger than the values found for $\text{Ba}(\text{Fe},\text{Ni})_2\text{As}_2$ [18, 36]. As the studied sample presents the SMP in isothermal $M(H)$ curves with maximum magnetization occurring at H_p (see the right inset of figure 6), it is unlikely that the VG phase exists below H_p , as the many explanations found for the SMP do not include a VG phase. On the other hand, exhaustive relaxation rate curves obtained in [21] in the same sample did not show any marked change as H_p was crossed. A similar result was observed for $\text{Ba}(\text{Fe},\text{Ni})_2\text{As}_2$ [36] where the maximum in the critical current, $J_c(H)$, occurring at H_p was explained in terms of a softening of the vortex lattice [37]. These facts motivated us to analyse the shape of $J_c(H)$ curves in our sample. We present in the inset of figure 7 the critical current calculated for selected $M(H)$ curves obtained in our sample [21] by using the Bean Model expression [38], $J_c = 20\Delta M/[a(1 - a/3b)]$ where $a < b$ are the sample dimensions perpendicular to the applied magnetic field and ΔM is the width of the hysteresis curves. As shown in this inset, the $J_c(H)$ curves show a broad region followed by a more well defined peak, which according to a theory developed in [37], might be explained in terms of a softening of the vortex lattice where in that case $J_c(H)$ in the peak region is given by $J_c(H) = A/[(B - B_p)^2 + (\Delta B)^2]^{5/4}$ where A , B_p and ΔB are fitting parameters, B_p is the peak position and ΔB is the peak width. The solid lines in each curve of the inset represent a fitting of the above expression to the peak, evidencing that the shape of the peaks can be well explained in terms of a softening of the vortex lattice. Results of the fitting parameters for the curves at $T = 20, 21$ and 22 K are $B_p = 53, 44$ and 36 kOe and $\Delta B = 33, 24$ and 19 kOe respectively. The values of B_p coincide with the corresponding H_p in each curve, and the values of ΔB are in agreement with those found in [36, 37]. Values of H_p corresponding to the peak in $J_c(H)$ curves are added to figure 7. As a VG phase is present below the T_g line, the latter further suggests that the softening is a precursor of an order-disorder transition taking place above the H_p line.

4. Conclusions

In conclusion, plots of the inverse logarithmic derivative of resistivity and of the third harmonic signal with temperature allowed the identification of a VG phase occurring below the glass temperature $T_g(H)$ in a high quality single crystal of the isovalently substituted iron pnictide $\text{BaFe}_2(\text{As}_{0.68}\text{P}_{0.32})_2$ with $T_c = 28.8$ K. From our knowledge this is the first study of the VG phase in an isovalently substituted iron pnictide, which are believed to be much cleaner systems when compared with hole and electron doped pnictides [39]. Plots of the inverse logarithmic derivative of ρ with temperature allowed us to identify a region exhibiting critical behaviour (and the corresponding critical exponent s) lying between T_g and the

temperature T^* above which a vortex–liquid phase takes place. The TAFF U_0 is extracted from the Arrhenius plot of resistivity. We successfully applied the modified VG model to our data where isochamp plots of the VG activation energy with temperature allowed the extraction of T_g , the temperature independent VG activation energy U_b , the temperature T^* marking the transition to the vortex liquid phase, and T_a which is close to $T_c(H)$. It is shown that isochamp plots of ρ/ρ_n versus t_s for $H \geq 2$ T collapses in a single curve where $t_s = (T/T_g)(T_a - T_g)/(T_a - T) - 1$ is a scaled temperature obtained from the modified VG model. Values of U_0 obtained from the TAFF model are found to be one order of magnitude larger than the VG activation energy U_b , but interestingly, values of U_b are of the same order of U_0 obtained from flux–creep measurements. A H_p line (corresponding to the peak in isothermal $J_c(H)$ curves and related to a softening of the vortex lattice) is added to the phase diagram as the lower border of the VG phase. The resulting T_g line was well fitted by a theoretical approach which considers the effect of disorder.

Acknowledgments

SSS and ADA acknowledge support from CNPq, JM and DS acknowledges the Spanish MICINN (grant No. FIS2016-79109-P), and the Xunta de Galicia (grants GPC2014/038 and AGRUP 2015/11). AC and AMI acknowledge support from the COST Action MP 1201 Nanoscale Superconductivity: Novel Functionalities through Optimized Confinement of Condensate and Fields, and from the Romanian Ministry of National Education and Research through Core Programme PN16-480102 Synthesis and characterisation of nanostructured materials, thin films and heterostructures; through PCCA 138/2012; and through POC Project P-37-697 nr. 28/01.09.2016. SS acknowledges a fellowship from CAPES, Science Without Borders program, project 88881.030498/2013-01. The work at IOP, CAS, is supported by NSFC (11374011 and 11374346) and CAS (SPRP-B: XDB07020300).

References

- [1] Rosenstein B and Li D 2010 *Rev. Mod. Phys.* **82** 109
- [2] Fisher D S, Fisher M P A and Huse D A 1991 *Phys. Rev. B* **43** 130
- [3] Bednorz J G and Müller K A 1986 *Z. Phys. B* **64** 189
- [4] Müller K A, Takashige M and Bednorz J G 1987 *Phys. Rev. Lett.* **58** 1143
- [5] Nattermann T and Scheidl S 2000 *Adv. Phys.* **49** 607
- [6] Rydh A, Rapp O and Andersson M 1999 *Phys. Rev. Lett.* **83** 1850
- [7] Andersson M, Rydh A and Rapp O 2001 *Phys. Rev. B* **63** 184511
- [8] Kamihara Y, Watanabe T, Hirano M and Hosono H 2008 *J. Am. Chem. Soc.* **130** 3296
- [9] Wen H H, Mu G, Fang L, Yang H and Zhu X 2008 *Europhys. Lett.* **82** 17009
- [10] Ren Z A et al 2008 *Europhys. Lett.* **82** 57002
- [11] Kim H J, Liu Y, Oh Y S, Khim S, Kim I, Stewart G R and Kim K H 2009 *Phys. Rev. B* **79** 014514
- [12] Ghorbani S R, Wang X L, Shabazi M, Dou S X, Choi K Y and Lin C T 2012 *Appl. Phys. Lett.* **100** 072603
- [13] Inosov D et al 2009 *Phys. Rev. B* **81** 014513
- [14] Shabazi M, Wang X L, Ghorbani S R, Ionescu M, Shcherbakova V, Wells F S, Pan A V, Dou S X and Choi K Y 2013 *Supercond. Sci. Technol.* **26** 095014
- [15] Choi K Y and Kim K 2013 *Prog. Supercond. Cryogenics* **15** 16
- [16] Prando G, Giraud R, Aswartham S, Vakaliuk O, Abdel-Hafiez M, Hess C, Wurmehl S, Wolter A U B and Büchner B 2013 *J. Phys.: Condens. Matter* **25** 505701
- [17] Hao F, Zhang M, Teng M, Yin Y, Jiao W, Cao G and Li X 2015 *IEEE Mag. Conf. INTERMAG* p 7157084
- [18] Salem-Sugui S Jr, Alvarenga A D, Luo H Q, Zhang R and Gong D L 2017 *Supercond. Sci. Technol.* **30** 015007
- [19] Lee H S, Bartkowiak M, Kim J and Lee H J 2010 *Phys. Rev. B* **82** 104523
- [20] Yu Y, Wang C, Li Q, Wang H and Zhang C 2014 *J. Phys. Soc. Jpn.* **83** 114701
- [21] Salem-Sugui S Jr, Mosqueira J, Alvarenga A, Sónora D S, Herculano E P, Hu D, Chen G and Luo H Q 2015 *Supercond. Sci. Technol.* **28** 055017
- [22] Kes P H, Aarts J, van den Berg J, van der Beek C J and Mydosh J A 1989 *Supercond. Sci. Technol.* **1** 242
- [23] Rosenstein B and Zhuravlev V 2007 *Phys. Rev. B* **76** 014507
- [24] Nakajima M, Uchida S, Kihou K, Lee C H, Iyo A and Eisaki H 2012 *J. Phys. Soc. Jpn.* **81** 104710
- [25] Crisan A, Iyo A and Tanaka Y 2003 *Appl. Phys. Lett.* **83** 506
- [26] Fabbriatore P, Farinon S, Gemme G, Musenich R, Parodi R and Zheng B 1994 *Phys. Rev. B* **50** 3189
- [27] Zhang Y Z, Ren Z A and Zhao Z X 2009 *Supercond. Sci. Technol.* **22** 065012
- [28] Shabazi M, Wang X L, Shekhar C, Srivastava O and Dou S 2010 *Supercond. Sci. Technol.* **23** 105008
- [29] Shabazi M, Wang X L, Lin Z W, Zhu J G, Dou S X and Choi K Y 2011 *J. Appl. Phys.* **109** 07E151
- [30] Zhou W, Zhuang J, Yuan F, Li X, Xing X, Sun Y and Shi Z 2014 *Appl. Phys. Exp.* **7** 063102
- [31] Shi D and Salem-Sugui S Jr 1991 *Phys. Rev. B* **44** 7647
- [32] Maley M P, Lessure J O W H and McHenry M 1990 *Phys. Rev. B* **42** 2639
- [33] Werthamer N R, Helfand E and Hohenberg P C 1966 *Phys. Rev.* **147** 295
- [34] Sundar S, Chandra L S S, Chattopadhyay M K and Roy S B 2015 *J. Phys.: Condens. Matter* **27** 045701
- [35] Gasparov V A, Drigo L, Audouard A, Sun D L, Lin C T, Bud'ko A L, Canfield P C, Wolff-Fabris F and Wosnitza J 2011 *Pis'ma v ZhETF* **93** 746
- [36] Salem-Sugui S Jr, Alvarenga A D, Rey R I, Mosqueira J, Luo H Q and Lu X Y 2013 *Supercond. Sci. Technol.* **26** 125019
- [37] Rosenstein B, Shapiro B Y, Shapiro I, Bruckental Y, Shaulov A and Yeshurun Y 2005 *Phys. Rev. B* **72** 144512
- [38] Bean C P 1964 *Rev. Mod. Phys.* **36** 31
- [39] Demirdis S, Fasano Y, Kasahara S, Terashima T, Shibauchi T, Matsuda Y, Konczykowski M, Pastoriza H and van der Beek C J 2013 *Phys. Rev. B* **87** 094506